J Solid State Electrochem (2017) 21:3495–3504
DOI 10.1007/s10008-017-3693-1

ORIGINAL PAPER

All-electrochemical approach for the assembly of platinum nanoparticles/polypyrrole nanowire composite with electrocatalytic effect on dopamine oxidation

Elisabetta Mazzotta[1,2] · **Antonio Caroli**[1] · **Elisabetta Primiceri**[3] · **Anna Grazia Monteduro**[3,4] · **Giuseppe Maruccio**[3,4] · **Cosimino Malitesta**[1]

Received: 13 June 2017 / Revised: 29 June 2017 / Accepted: 30 June 2017 / Published online: 14 July 2017

Abstract In the present study, a composite material consisting of polypyrrole nanowires (PPyNWs) and platinum nanoparticles (PtNPs) has been developed by an all-electrochemical approach and proved to be highly effective for electrochemical determination of dopamine (DA). PPyNWs are electropolymerized by a template-free method, and PtNPs are subsequently electrodeposited by cyclic voltammetry. Chemical characterization by X-ray photoelectron spectroscopy showed the effective PtNP immobilization on polymer nanowires discriminating at the same time Pt species deposited and revealing the occurrence of polypyrrole-PtNP interaction. The morphology of the composite material was characterized using scanning electron microscopy that showed spherical Pt nanoparticles well distributed within PPy-NW network. DA detection was performed by differential pulse voltammetry technique obtaining satisfactory performances in terms of linear range (1–77 μM), sensitivity, reproducibility (RSD 2.7%), and detection limit (0.6 μM). The electrocatalytic role of PtNPs in DA electroxidation process is clearly demonstrated by the comparison with PPyNWs only. Moreover, no significant response is observed in the presence of common interference as ascorbic acid and uric acid, which may coexist with DA in biological fluids, demonstrating a good selectivity toward DA. Moreover, DA was detected in human serum samples spiked obtaining a satisfactory recovery of 94%. A synergistic effect involving both PtNPs and PPyNWs is invoked for explaining the observed electrocatalytic activity.

✉ Elisabetta Mazzotta
elisabetta.mazzotta@unisalento.it

[1] Dipartimento di Scienze e Tecnologie Biologiche ed Ambientali, Università del Salento, Via Monteroni, 73100 Lecce, Italy

[2] IFAC-CNR, Via Madonna del Piano, 10–50019 Sesto Fiorentino, FI, Italy

[3] CNR NANOTEC-Institute of Nanotechnology c/o Campus Ecotekne, Via Monteroni, 73100 Lecce, Italy

[4] Dipartimento di Matematica e Fisica, Università del Salento, Via per Arnesano, 73100 Lecce, Italy

Introduction

Dopamine (DA), one of the most significant neurotransmitters in the central nervous system, plays an important role in several aspects of brain circuitry, neuronal plasticity, and control of stress responses. Low levels of DA are implicated as a major cause of neurological diseases, such as schizophrenia and Parkinson's disease. It is therefore important to develop methods that enable effective quantification of DA. Since DA is an electrochemically active compound, many examples of electrochemical sensors have been reported in literature for its detection [1], also due to inherent advantages of electrochemical methods, such as low cost, rapid response, sensitivity, and easy miniaturization. In particular, efforts have been oriented through the development of selective electrode coatings to remove DA interferences rejecting other electroactive compounds that usually coexist at high concentrations. One of the strongest DA interferences is ascorbic acid (AA) whose redox potential is very close to that of DA at physiological pH. Moreover, AA in vivo concentration can be 3–4 orders of magnitude higher than the concentration of DA [2]. That is why a widely used approach for DA electrochemical detection consists in the use of chemically modified electrodes by employing materials able to selectively interact with DA rejecting other electroactive compounds [3–6]. Among these, permselective membranes have become a fascinating approach for DA selective recognition. Being DA

(pK_a = 8.92), a cation at physiological pH, while AA (pK_a = 4.10) is an anion [7], a film presenting a cationic permselectivity can thus interact with DA and act as a barrier to hinder the diffusion of anions. During the last years, a large variety of polymeric film has been proposed to this aim, including poly(o-phenylendiamine) [8], poly(hippuric acid) [9], poly(4-amino-1,1′-azobenzene-3,4′-disulfonic acid) [10], poly(3,4-ethylendioxythiophene-co-(5-amino-2-naphthalenesulfonic acid) [11], and Nafion/CdSe/polyaniline [12]. In other cases, polymer-modified electrodes revealed to be able to detect simultaneously DA, AA, and other anionic interferences due to the achieved separation between their redox potentials [13–15]. In this context, a widely used polymeric material is polypyrrole (PPy), particularly in its overoxidized state, possessing excellent cation permselectivity due to negatively charged functionalities acquired during the overoxidation process. Nonetheless, also doped PPy has been demonstrated to selectively detect DA allowing obtaining well-separated peaks for the analyte and for its interferences [16]. While the use of PPy is a well-consolidated approach in this field, a more recent research trend is focused on PPy nanostructuring and on its sensing applications, with the aim of exploiting advantages related to transition from the bulk scale to the nanoscale, mainly consisting in combining PPy properties, such as cation permselectivity, high electronic conductivity, good stability in aqueous solutions, and biocompatibility with ones of nanomaterials, such as large surface area, size, and quantum effect [17–19]. Several examples of PPy nanostructures have been developed and successfully applied in DA electrochemical detection [20, 21].

In most cases, the assembly of composite materials integrating polymer nanostructures and metal nanoparticles (NPs) has been demonstrated to determine a further improvement of sensor performances due to the additional generated electrocatalytic sites between NPs dispersed into the polymer and the skeleton of PPy [22, 23]. Such improvement derives also from the high dispersion of metal nanoparticles promoted by polymer nanostructure, which in turn determines enhanced metal electrocatalytic activity. These aspects give an idea of the crucial role played by PPy nanostructure as well as by experimental conditions used for metal deposition, which should determine homogeneous deposition of highly dispersed metal NPs, thus allowing their high metal catalytic activity to be fully achieved.

In the present work, a novel electrochemical sensor for DA is proposed based on an all-electrochemical, easy, rapid, and low-cost approach for the integration of PPy nanowires (PPyNWs) with platinum nanoparticles (PtNPs). Although several reports explored the development of composite system nanosized PPy/metal NPs for electrocatalytic applications [24–29], to the best of our knowledge, the integration of PPy nanowires with PtNPs as a catalytic system for the electroxidation of DA was not reported before. Only recently, Ghadimi et al. [30] developed an electrochemical sensor for DA, based on the integration of PPy nanosheet with Pt nanoparticles. The authors adopted a chemical synthesis of PPy nanosheet followed by Pt deposition by chemical reduction process and subsequent drop casting of the mixture on the electrode surface, resulting in a time-consuming (more than 48 h) multistep temperature-controlled process. In the present work, an all-electrochemical approach is used for the assembly of composite material allowing the simple and rapid deposition of both PPy nanowires and PtNPs directly on the electrode surface with good adherence and high homogeneity.

Moreover, PPyNWs are electrochemically synthesized by using a simple templateless approach [31] which, contrarily to template-assisted electrochemical techniques, has the significant advantages of not requiring any hard or soft templating structures, thus providing a higher degree of flexibility in defining morphology at nanoscale, along with a time reduction, being eliminated template functionalization and removal steps, before and after electropolymerization, respectively. Additionally, the proposed template-free approach is very simple, rapid, and green requiring the use of only aqueous solutions. A polymeric nanostructured matrix with highly accessible surface area is thus achieved which favors deposition of highly dispersed metal nanoparticles. PtNPs, selected for their reported ability of accelerate redox kinetics on electrode surface [32], are synthesized by electrochemical deposition which provides a good control of growth process as the driving force for metal formation (i.e., the electrode potential) can be controlled more precisely and on a much shorter timescale than in alternative processes such as chemical reduction. In particular, PtNPs are electrochemically deposited on PPyNWs by cyclic voltammetry, which enables the deposited Pt particles to be activated periodically and improves their dispersion [33]. Moreover, cyclic voltammetry (CV) deposition gives the possibility of (real-time) monitoring platinum deposition process allowing also to identify and tune experimental parameters possibly influencing it (i.e., scan rate, cycle number, potential window).

An additional advantage of the proposed all-electrochemical approach thus relies in the possibility of effectively combining the effect of cyclic potential with that of polymeric nanowire network in promoting PtNP dispersion, resulting in a composite matrix with nanoparticles embedded within and firmly anchored, as shown by morphological characterization by scanning electron microscopy (SEM). Chemical investigation by X-ray photoelectron spectroscopy (XPS) evidenced not only the successful platinum deposition, but also providing useful information about its oxidation state, but, interestingly, it allowed us to postulate a possible involvement of pyrrole nitrogen in the platinum deposition process. The as-developed PPyNW/PtNP system was successfully applied to DA detection, revealing its ability to selectively detect

DA in presence of interfering molecules with satisfactory performances, also in real sample analysis. The key electrocatalytic role of PtNPs in DA electroxidation process is clearly demonstrated by the comparison with PPyNWs only. Starting from the description of DA electroxidation pathway, a possible mechanism for explaining the electrocatalytic role of PtNPs is proposed in a synergistic effect involving also the contribution of polymeric nanowire matrix.

Experimental

Pyrrole and all other reagents were purchased from Sigma and used as received. Ultrapure water (Millipore Milli-Q, 18.2 MΩ/cm) was used.

Electrochemical experiments were carried out with a CHI 660D Potentiostat (CH Instruments) controlled by a computer. A one-compartment three-electrode cell was used, consisting of a glassy carbon disc (diameter 3 mm), a platinum wire, and a saturated calomel electrode (SCE) as working, counter, and reference electrodes, respectively.

PPyNW electropolymerization was performed from a solution of pyrrole 0.1 M in K_2HPO_4 0.2 M solution (pH adjusted to 6.8 by adding NaOH) containing $LiClO_4$ 0.07 M by applying a constant potential of 0.85 V (vs SCE) until a charge of 0.43 C/cm^2 was circulated. PPyNWs were then cycled for 10 cycles from −0.25 to 1.2 V in H_2SO_4 0.5 M, scan rate 50 mV/s. Pt deposition was carried out by CV from 0.4 to −0.25 V for 20 cycles in H_2SO_4 0.5 M containing H_2PtCl_6 10 mM, scan rate 10 mV/s.

DA electrochemical detection was performed by differential pulse voltammetry (DPV) between −0.1 and 0.4 V with a step potential of 2 mV, a modulation amplitude of 50 mV, and a scan rate of 10 mV/s, in phosphate buffer solution (PBS) 0.1 M, pH 7.0. Selectivity studies were carried out by DPV analysis of DA 120 μM in presence of ascorbic acid (AA) 750 μM, and uric acid (UA) 750 μM. DA was detected under the same experimental conditions in spiked samples of human serum, after 30 times dilution with PBS buffer.

The morphology of PPyNW samples and composite system PPyNWs/PtNPs was investigated by scanning electron microscopy (SEM, Carl Zeiss Merlin) with an accelerating voltage of 5 kV. SEM images were acquired through an in-lens detector for secondary electrons in top-view configuration. Image analysis has been performed by using the ImageJ 1.49v (National Institutes of Health, USA) software in order to evaluate the diameter of the PPy nanowires and Pt nanoparticles.

XPS measurements were performed using an Axis ULTRA DLD spectrometer (Kratos Analytical, UK) with a monochromatic Al Kα source operating at 225 W (15 kV, 15 mA). For each sample, a wide-scan spectrum is acquired in the binding energy range 0–1200 eV with a pass energy of 160 and 1 eV step, while high-resolution regions were acquired with a pass energy of 20 and 0.1 eV step. In both cases, the area of analysis is about 700 × 300 μm^2. The base pressure in the instrument was 1 × 10^{-9} mbar. Data analysis was performed by the CasaXPS software (version 2.3.16). Surface charging was corrected considering adventitious C 1s (binding energies (BE) = 285 eV).

Results and discussion

PtNP deposition by cyclic voltammetry

Figure 1 reports voltammetric curves recorded during PtNP electrochemical deposition on PPy nanowires (20 cycles). It can be clearly observed the presence of a pair of current peaks between −0.2 and 0.0 V, which are due to hydrogen adsorption and desorption processes at Pt particles [34]. The appearance of such redox peaks since the fourth cycle suggests that the Pt deposition process is rapidly initiated with cyclic potential. They are more and more pronounced with the increasing of cycle number evidencing that, as expected, the platinum loading can be controlled with increasing deposition time/cycle numbers. Redox current increase can be still observed during the last cycles, although to a lower extent, suggesting the possibility of further increasing platinum loading after 20 scans, in these experimental conditions. Nonetheless, as it will be discussed later (see "DA detection by DPV. Selectivity test" section), this does not imply an improvement of catalytic properties of the resulting composite system probably due to particle aggregation phenomena. It is interesting to highlight that the electrochemical behavior of PtNP described by CV in Fig. 1 is similar to that of Pt particles on metal and carbonaceous supports confirming that, as previously reported [31], PPy nanowires grown under the adopted electrochemical conditions possess high electronic conductivity and good charge transport properties allowing the effective Pt deposition to be easily achieved.

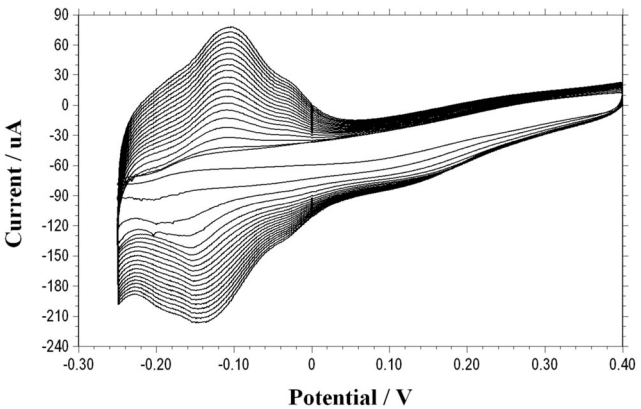

Fig. 1 Cyclic voltammetry in H_2SO_4 0.5 M for the electrodeposition of PtNPs on PPyNWs. H_2PtCl_6 10 mM, scan rate 10 mV/s, and 20 cycles

Morphological characterization of PPyNWs/PtNPs

SEM images of bare PPy nanowires and of the PPyNW/PtNP composite system are shown in Fig. 2. As clearly evidenced in Fig. 2a, b, the adopted templateless approach leads to the formation of a high-density PPyNW network with a narrow nanowire diameter distribution of 60 ± 10 nm and a highly homogeneous coverage of the electrode surface. The high aspect ratio of polymer nanowires contributes to create a high-surface-area tridimensional "open" structure, particularly suitable for nanoparticle deposition/dispersion. On the other hand, the PPyNW/PtNP composite system exhibits a major change in the morphology. Indeed, Fig. 2d shows almost spherical platinum cluster and nanoparticles with diameters ranging from 500 to 40 nm, chiefly located on nanowire tips/turns. At a higher magnification (Fig. 2c), the smaller nanoparticles (diameter range 65 ± 20 nm) are better visible to form an intimately connected structure with the underlying nanowire network in the region closer to the electrode surface. The cluster with higher diameter (in the range 350 ± 100 nm) instead protrudes in the upper region toward the interface with the solution. This distribution could suggest that during the first scans, platinum deposition starts in positions where the local charge amount is higher (such as nanowire tips/turns). In successive scans, such a local charge accumulation could be gradually attenuated from platinum deposition, making the entire nanowire surface equally suitable for particle deposition. Alternatively, platinum reduction could just occur faster in the regions with higher charge density bringing to a major growth there. In both cases, this would result in a further diameter increase for firstly deposited or faster-growing particles, which merge originating clusters up to 500 nm, in addition to the smaller nanoparticles. Increasing the number of scans (from 20 to 100 scans, results not shown), further platinum deposition determines the formation of larger deposits resulting in a bulk platinum structure covering the underlying nanowire/nanoparticle network.

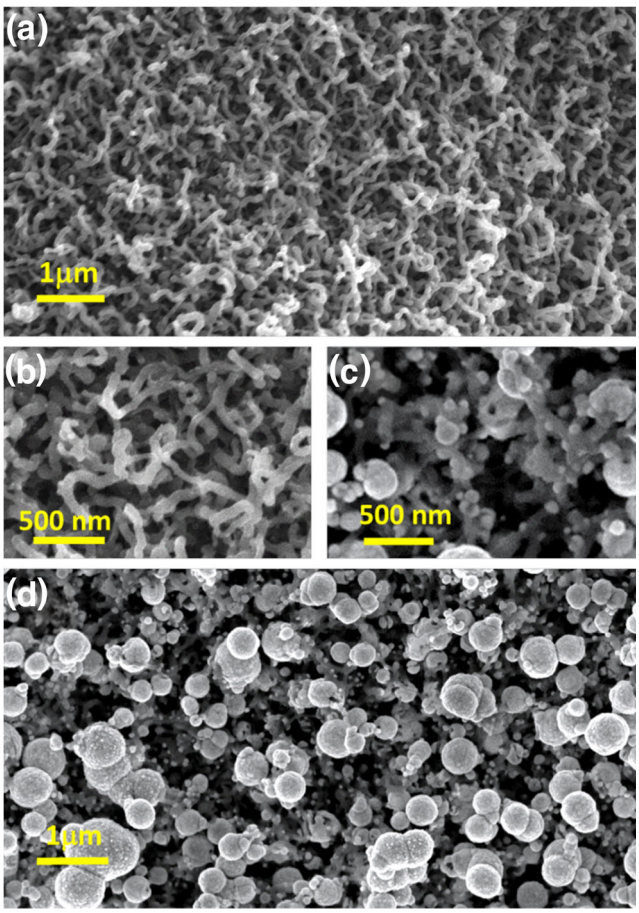

Fig. 2 SEM top-view images of PPyNWs (**a**, **b**) and of the composite system PPyNWs/PtNPs (**c**, **d**)

XPS characterization of PPyNWs/PtNPs

XPS was employed to analyze the chemical composition and status of the composite system PPyNWs/PtNPs. Figure 3 presents detailed spectrum recorded in Pt 4f region and clearly shows two main peaks at 71.4 and 74.7 eV, corresponding to Pt 4f7/2 and 4f5/2, respectively. In detail, composite system appears to be characterized by three chemically different Pt species, corresponding to metallic Pt(0) with BE of 71.4 and 74.7 eV, oxide Pt(II) with BE of 72.2 and 75.4 eV, and oxide Pt(IV) with BE of 73.4 and 76.4 eV, respectively. The anchored Pt species are predominantly in the metallic state. The presence of a small amount of oxidized Pt species (Pt(II) and Pt(IV)) with the peak area of about 35% may be ascribed to the incomplete reduction of the Pt species. For a comparison, XPS analysis on PPyNWs alone was also performed. An interesting feature emerging from the comparison

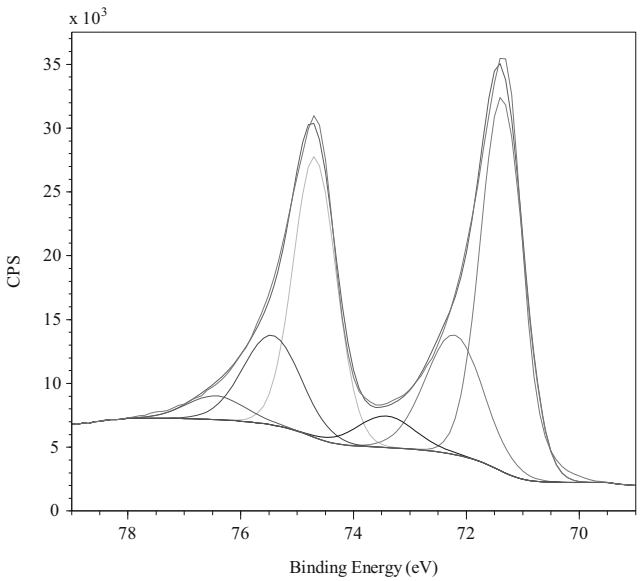

Fig. 3 Pt 4f high-resolution XPS spectrum on PPyNWs/PtNPs with curve fitting results. Spectra are charging corrected

of two samples can be drawn from N 1s signal, reported in Fig. 4 for PPyNWs (Fig. 4a) and for PPyNWs/PtNPs (Fig. 4b). In PPyNW sample, four components can be identified located at 398.35, 400.23, 401.73, and 402.66 eV and assigned, respectively, to C=N, pyrrole –NH–, C–N^+, and C=N^+, which are typical features of PPy film [35]. After PtNP deposition, an evident decrease of N 1s signal intensity occurs (Fig. 4b), ascribable to PtNP deposition on nanowire matrix, partially covering it. Although the same four components can be identified, located at 398.78, 400.1, 401.62, and 402.48 eV, a remarkable variation of N 1s spectrum is observed, mainly consisting in the attenuation of pyrrole –NH– component, with subsequent modification of percentage area of other components. This could be tentatively explained hypothesizing that PtNPs preferentially interact with pyrrolic nitrogen: NH moieties in the polymer structure could act as localized chemically active sites for the enhanced anchoring of metal nanoparticles [36]. Interaction between pyrrole and PtNPs is reported [37] to be likely that of zerovalent platinum with conjugated dienes, with the addition of σ-bonding to the nitrogen atom, with the corresponding polymer expected to form more stable bonding.

Such a result further confirms the high suitability of PPy as polymeric matrix for PtNP deposition and its key role in the process due to three concomitant effects, which can be summarized as follows: firstly, the three-dimensional high-surface-area structure formed by nanowire assembly promotes nanoparticle dispersion; secondly, PPy conductive nature allows the electrochemical deposition of PtNPs to be achieved with an effect on their size/distribution; thirdly, the occurrence of chemical interaction between PPy and PtNPs enables the formation of stable PtNP deposition, crucial aspect for any desired catalytic application of the composite material.

DA detection by DPV. Selectivity test

The electrocatalytic activity of PPyNW/PtNP composite system toward DA electrochemical oxidation has been investigated by DPV measurements. Results are reported in Fig. 5. It is evident that the system exhibits a linear response to DA in the concentration range 1–77 μM, as shown by the calibration curve in Fig. 5b (diamond points)—whose equation is $i_p(\mu A) = (0.125 \pm 0.005)[DA](\mu M) + (3.78 \pm 0.21)$—with a sensitivity of (0.125 ± 0.005) μA/μM ($R = 0.994$) and a LOD value equal to 0.6 μM (S/N = 3). Moreover, a good interelectrode reproducibility is observed (RSD 2.7%, $n = 3$) evidencing the reliability of the experimental conditions for the assembly of composite systems, thus confirming the high relevance of the adopted all-electrochemical approach.

From DPV curves in Fig. 5a, it is interesting to observe the value of peak potential (about 0.15 V vs SCE), which is significantly lower than DA oxidation potential typically observed both on bare and on modified electrodes [22, 38], between 0.3 and 0.4 V. This is due to the electrocatalytic effect of PtNPs, which play a key role in enhancing DA oxidation process resulting in oxidation current increase and in lowering oxidation potential value, as demonstrated by the comparison with calibration curve recorded, under the same experimental conditions, on PPyNWs (Fig. 4b, square points). Also PPyNWs exhibit a certain current response to DA although a lower sensitivity (0.098 μA/μM, $R = 0.997$) is observed mon-

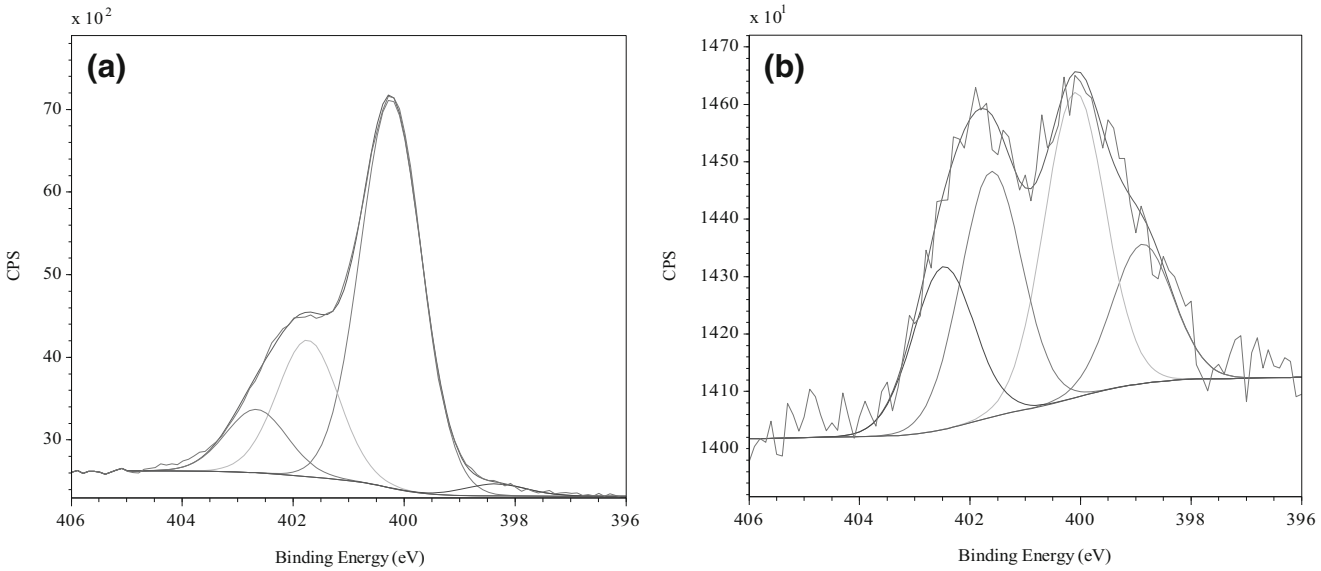

Fig. 4 N 1s high-resolution XPS spectrum on PPyNWs (**a**) and on PPyNWs/PtNPs (**b**) with curve fitting results. Spectra are charging corrected

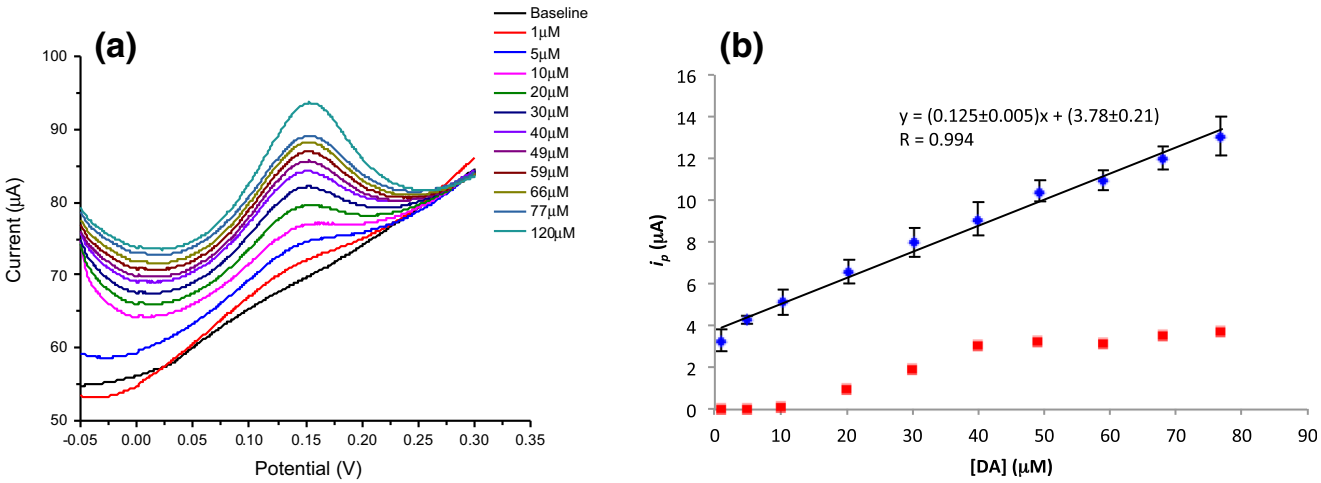

Fig. 5 **a** DPV curves recorded on PPyNWs/PtNPs exposed to different DA concentrations (1–120 μM) in PBS 0.1 M pH 7.0. Step potential 2 mV, modulation amplitude 50 mV, and scan rate 10 mV/s. **b** DA calibration curve on PPyNWs/PtNPs (*diamond*) and on PPyNWs (*squares*)

itoring i_p at 0.15 V, with a very narrow linear range (10–40 μM). DA electroxidation process on Pt nanoparticles can be assumed to proceed, similarly to what was reported on Pt electrodes [39], following a four-electron process with an ECE mechanism, which consists of three steps: Faradaic oxidation to the quinone, ring closure and regeneration of the catechol, and Faradaic reoxidation to the quinone. As reported in Scheme 1, DA (I) is oxidized by a two-electron process to the DA-*o*-quinone (II), which is unstable and rearranges by cyclization to the indole, leukoaminochrome (III). This is further oxidized by a two-electron step, with the product being a mixture of the tautomers, aminochrome (IV), and 5,6-dihydroxyindole (V), the proportion of V increasing with increasing pH. Further, the cyclized catechol, III, is more easily oxidized than the open-chain catechol, I, and is chemically oxidized by the *o*-quinone, II, with formation of I and IV. As in the case of Pt bulk electrodes, such a reaction mechanism can be expected to take place on the surface of Pt

Scheme 1 The ECE mechanism for DA oxidation. *E* denotes the electrochemical reactions while *C* denotes the chemical reactions

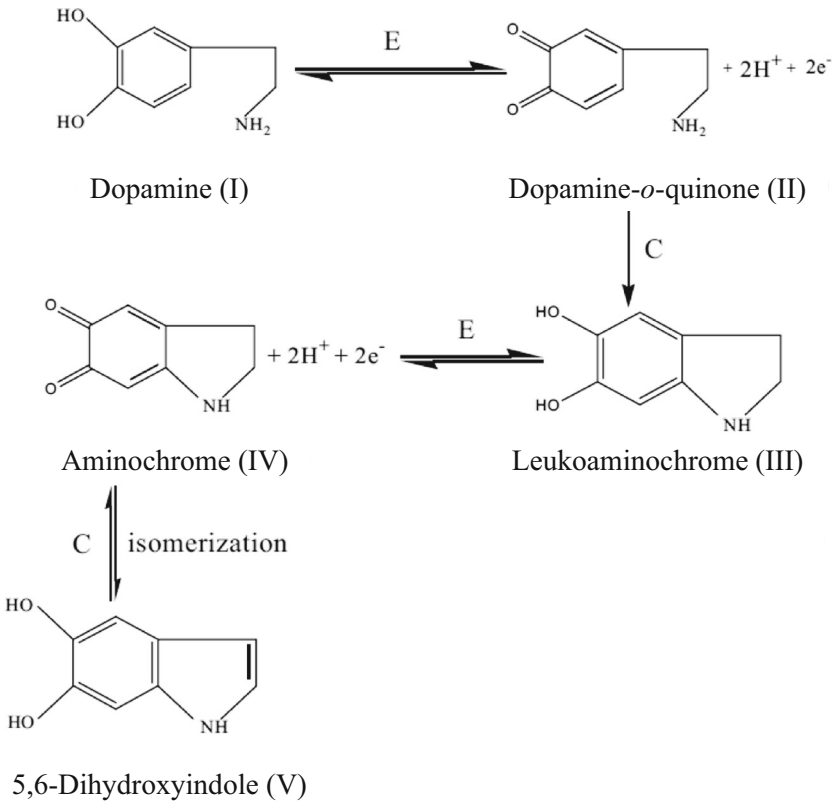

nanoparticles, taking advantage of the nanosize range determining a significant increase of the surface area exposed to the analyte, in a situation approaching the homogeneous catalysis case, with a subsequent increase of oxidation current. Moreover, PtNPs could play also another role in the electrocatalysis of DA oxidation which could occur, as in the case of other organic compounds [40], by a mechanism catalyzed by the anodic formation of Pt oxides (Pt(OH), PtO), proceeding with the discharge of H_2O to produce adsorbed hydroxyl radicals by the reaction: $Pt + H_2O = Pt(OH) + H^+ + e^-$. In addition, an extensive DA adsorption is expected to occur on reduced Pt surface [40], further promoted by Pt high-surface nanostructure. The overall DA oxidation reaction could thus involve the interaction between anodically generated Pt oxides and Pt-adsorbed DA in a surface-catalyzed oxidation process following reactions described in Scheme 1 and producing Pt(0) with subsequent regeneration of Pt oxide catalyst at the working potential.

It should be remarked that also PPyNWs play a crucial role in such a catalytic process, with the result that the observed electrocatalytic activity has to be ascribed to the synergistic effect of each component of the composite material. On one hand, as discussed above, PPy nanowires, due to their structure/conductivity properties, promote the deposition of nanosized and highly dispersed Pt particles, which have a major role in catalytic process. On the other hand, polymer matrix plays another more direct effect on the electrocatalytic activity of the composite material due to polymer-catalyst electronic interaction [41, 42], contributing to reduce reaction overpotentials.

DPV experiments evidenced that the electrocatalytic performances of PPyNWs/PtNPs are not improved by modifying the cycle number in Pt deposition. Systems prepared under the same experimental conditions but with lower (i.e., 10) and higher (i.e., 100) cycle number exhibited a significantly lower DPV current response to DA 120 μM, equal to, respectively, 56 and to 20% of the current response recorded on system prepared by 20 scans. The current response obtained in the former case could be reasonably due to the deposition of a lower amount of Pt nanoparticles, exhibiting a less remarkable catalytic activity. On the other hand, in the latter case, the increase of Pt loading results in a poorer sensor response, which could be due to the hypothesized mechanism of Pt deposition described in the "Morphological characterization of PPyNWs/PtNPs" section. With the increase of scan number, Pt nanoparticles on nanowire tips could aggregate forming larger clusters covering underlying nanowire/nanoparticle network, thus acting as bulk Pt and nullifying the nanosize effect. Such results show that the adopted experimental conditions allow getting a trade-off between the deposition of few rare Pt nanoparticles and larger Pt cluster, where Pt nanoparticles, with at least two distinct size distributions, coexist and are well dispersed on/within PPy nanowires. This morphology of the resulting composite system evidently allows a synergistic effect to be achieved in electrocatalytic DA oxidation.

A comparison between results obtained in DA electrochemical detection with the developed sensor and other recently reported sensors based on composite systems integrating metal nanoparticles is listed in Table 1. The proposed

Table 1 Comparison of DA sensing performances of the developed PPyNW/PtNP system with other composite systems based on metal nanoparticles

Electrode material	Method	Linear range (μM)	LOD (μM)	Ref
AgNPs/PPy nanofiber	Cyclic voltammetry	0.5–155	0.1	[43]
AuNPs/PPy nanotubes	Square wave voltammetry	0.025–2.5	0.01	[44]
AuNPs/PPy nanoplates	Amperometry	1–5.2	0.36	[45]
AuNPs/NiO/poly(pyrrole-N-propionic acid)/tyrosinase	Electrochemical impedance spectroscopy	80–200	5.46	[46]
AuNPs/polydopamine	DPV	4–200	3.4	[47]
AuNPs/poly(4-thiophen-3-yl-aniline)	Amperometry	3–18	3	[48]
AuNPs/reduced graphene oxide/RNA aptamer	Cyclic voltammetry	0.5–20	0.13	[49]
PdNPs/Nafion/laccase	Amperometry	5–167	1.26	[50]
AuNPs/TiO_2 NPs/carbon nanotube	–	0.3–15	0.2	[51]
PdNPs/fullerene	DPV	0.35–133.35	0.056	[52]
CeO_2NPs/graphene nanosheet/Nafion	Electrochemical impedance spectroscopy	10–780	1	[53]
PtNPs/PPy nanosheets	DPV	0.01–400	0.0067	[30]
TiO_2NPs/2,2-[1,7-hepthandiylbis(nitriloethylidyne)]-bis-hydroquinone	Square wave voltammetry	1–6 8–1400	0.84	[54]
PPyNWs/PtNPs	DPV	1–77	0.6	This work

Table 2 Determination of DA in spiked human serum samples ($n = 3$)

Added (μM)	Found (μM)	Mean recovery (%)	RSD (%)
70	67.1		
70	64.5	94	2.1
70	66.6		

Experimental condition for DPV measurements as in Fig. 4

system exhibits comparable analytical performance in terms of detection limit and linear range. Nonetheless, in such a comparison, peculiar features of the developed system, related to the all-electrochemical route employed, such as low cost, simple, and rapid preparation, should be taken into account, which contribute to make it an effective system for monitoring DA.

The effect of AA and UA on DPV detection of DA was investigated by monitoring the current response to DA 120 μM in the presence of AA and UA 750 μM. Only a slight modification of DA current response was observed with an increase of peak current of 12% and a decrease of 6% in the presence of AA and UA, respectively, indicating a negligible interfering effect in both cases.

Real sample analysis

To validate the method in the analysis of DA in biological fluids, the system PPYNWs/PtNPs was further tested for DPV detection of DA in spiked human serum samples. Results are presented in Table 2. A satisfactory mean recovery of 94% is achieved with good sensor response reproducibility (RSD 2.1%), comparable with that obtained analyzing DA standard solutions. These findings evidence sensor reliability and applicability in monitoring DA in complex biological samples.

Conclusions

A new composite system PPyNWs/PtNPs was assembled by using a simple, low-cost, and rapid all-electrochemical approach. Morphological characterization by SEM provided evidence of PtNPs evenly distributed on/within PPy nanowire network, while chemical investigation by XPS gave information about oxidation state of deposited Pt, suggesting also a possible involvement of pyrrolic nitrogen in the platinum deposition process, thus evidencing that PPyNWs not only create a high-surface 3D structure which promotes PtNP dispersion with an effect on their size/distribution, but also act as a supporting material interacting with metal nanoparticles.

The electrocatalytic activity of the system toward DA oxidation was tested by DPV measurements, gaining satisfactory results in terms of LOD, linear range, sensitivity, and anti-interfering effects, as demonstrated by DPV investigation of DA in presence of AA and UA and by real sample analysis. A synergistic effect is invoked for explaining the observed electrocatalytic activity in DA oxidation process, involving both PtNPs and PPyNWs, with the former exhibiting enhanced catalytic activity due to nanosize and the latter playing an indirect effect related to its structure/conductivity, which influence Pt nanosize/dispersion, and in a direct effect related to electronic interaction polymer-catalyst.

Acknowledgements This activity was funded by the Italian Ministry of University and Research (MIUR) Futuro in Ricerca (FIR) programme under Grant no. RBFR122KL1 (SENS4BIO) and by Italian Ministry of University and Research (MIUR) through the project PRIN2015 "Multiple equilibria in natural and biological fluids: from speciation to selective sequestering" (code 2015MP34H3_004).

References

1. Hasanzadeh M, Shadjou N, de la Guardia M (2017) Current advancement in electrochemical analysis of neurotransmitters in biological fluids. TrAC Trends Anal Chem 86:107–121
2. Hsueh C, Brajter-toth A (1994) Electrochemical preparation and analytical applications of ultrathin overoxidired polypyrrole films. Anal Chem 66:2458–2464
3. Kang J, Zhuo L, Lu X, Wang X (2005) Electrochemical behavior of dopamine at a quercetin-SAM-modified gold electrode and analytical application. J Solid State Electrochem 9:114–120
4. Jin GP, Lin XQ, Ding YF (2006) Glassy carbon electrodes modified with mixed covalent monolayers of choline, glycine, and glutamic acid for the determination of phenolic compounds. J Solid State Electrochem 10:987–994
5. Ti CC, Kumar SA, Chen SM (2009) Electrochemical preparation, characterization, and electrocatalytic studies of Nafion-ruthenium oxide modified glassy carbon electrode. J Solid State Electrochem 13:397–406
6. Yang S, Li G, Yang R, Xia MQL (2011) Simultaneous voltammetric detection of dopamine and uric acid in the presence of high concentration of ascorbic acid using multi-walled carbon nanotubes with methylene blue composite film-modified electrode. J Solid State Electrochem 15:1909–1918
7. Zhang S, Xu Q, Zhang WJL (2001) In vivo monitoring of the monoamine neurotransmitters in rat brain using microdialysis sampling with liquid chromatography electrochemical detection. Anal Chim Acta 427:45–53
8. Mo J-W, Ogorevc B (2001) Simultaneous measurement of dopamine and ascorbate at their physiological levels using voltammetric microprobe based on overoxidized poly(1,2-phenylenediamine)-coated carbon fiber. Anal Chem 73:1196–1202
9. Zhao H, Zhang Y, Yuan Z (2002) Determination of dopamine in the presence of ascorbic acid using poly(hippuric acid) modified glassy carbon electrode. Electroanalysis 14:1031
10. Kumar SA, Tang C-F, Chen S-M (2008) Poly(4-amino-1-1′-azobenzene-3, 4′-disulfonic acid) coated electrode for selective detection of dopamine from its interferences. Talanta 74:860–866
11. Balamurugan A, Chen S-M (2007) Poly(3,4-ethylenedioxythiophene-co-(5-amino-2-naphthalenesulfonic acid)) (PEDOT-PANS) film modified glassy carbon electrode for selective detection of dopamine in the presence of ascorbic acid and uric acid. Anal Chim Acta 596:92–98

12. Shieh Y, Lu Y, Wang T, Yang CLR (2014) Electrocatalytic activities of Nafion/CdSe/self-doped polyaniline composites to dopamine, uric acid, and ascorbic acid. J Solid State Electrochem 18:975–984
13. Li NB, Ren W, Luo HQ (2008) Simultaneous voltammetric measurement of ascorbic acid and dopamine on poly(caffeic acid)-modified glassy carbon electrode. J Solid State Electrochem 12:693–699
14. Zhang L, Shi Z, Lang Q (2011) Fabrication of poly(orthanilic acid)-multiwalled carbon nanotubes composite film-modified glassy carbon electrode and its use for the simultaneous determination of uric acid and dopamine in the presence of ascorbic acid. J Solid State Electrochem 15:801–809
15. Zhang L, Wang L (2013) Poly(2-amino-5-(4-pyridinyl)-1, 3, 4-thiadiazole) film modified electrode for the simultaneous determinations of dopamine, uric acid and nitrite. J Solid State Electrochem 17:691–700
16. Saraceno RA, Pack JG, Ewing AG (1986) Catalysis of slow charge transfer reactions at polypyrrole-coated glassy carbon electrodes. J Electroanal Chem 197:265–278
17. Li C, Bai H, Shi G (2009) Conducting polymer nanomaterials: electrosynthesis and applications. Chem Soc Rev 38:2397–2409
18. Yoon H, Jang J (2009) Conducting-polymer nanomaterials for high-performance sensor applications: issues and challenges. Adv Funct Mater 19:1567–1576
19. Surdo S, Strambini LM, Malitesta C, Mazzotta E, Barillaro G (2012) Highly conformal growth of microstructured polypyrrole films by electrosynthesis on micromachined silicon substrates. Electrochem Commun 14:1–4
20. Rui Z, Huang W, Chen Y, Zhang K, Cao Y, Tu J (2017) Facile synthesis of graphene/polypyrrole 3D composite for a high-sensitivity non-enzymatic dopamine detection. J Appl Polym Sci 134:44840
21. Qian T, Yu C, Wu S, Shen J (2013) In situ polymerization of highly dispersed polypyrrole on reduced graphite oxide for dopamine detection. Biosens Bioelectron 50:157–160
22. Stoytcheva M, Zlatev R, Velkova Z, Gochev V, Montero G, Toscano L, Olivas A(2017) Advances in the electrochemical analysis of dopamine. Curr Anal Chem 13:89–103
23. Sajid M, Nazal MK, Mansha M, Alsharaa A, Muhammad S, Jillani S, Basheer C (2016) Chemically modified electrodes for electrochemical detection of dopamine in the presence of uric acid and ascorbic acid: a review. TrAC Trends Anal Chem 76:15–29
24. Poletti Papi MA, Caetano FR, Bergamini MF, Marcolino-Junior LH (2017) Facile synthesis of a silver nanoparticles/polypyrrole nanocomposite for non-enzymatic glucose determination. Mater Sci Eng C 75:88–94
25. Sharma P, Radhakrishnan S, Jayaseelan SS, Kim B-S (2016) Non-enzymatic electrochemical oxidation based on AuNP/PPy/rGO nanohybrid modified glassy carbon electrode as a sensing platform for oxalic acid. Electroanalysis 28:2626–2632
26. Chen J, Sheng Q, Zheng J (2015) Dispersed gold nanoparticles on NiO coated with polypyrrole for non-enzymic amperometric sensing of glucose. RSC Adv 5:105372–105378
27. Xing L, Rong Q, Ma Z (2015) Non-enzymatic electrochemical sensing of hydrogen peroxide based on polypyrrole/platinum nanocomposites. Sensors Actuators B Chem 221:242–247
28. Lin M (2015) A dopamine electrochemical sensor based on gold nanoparticles/over-oxidized polypyrrole nanotube composite arrays. RSC Adv 5:9848–9851
29. García-Hernández C, García-Cabezón C, Medina-Plaza C, Martín-Pedrosa F, Blanco Y, de Saja JR-MM (2015) Electrochemical behavior of polypyrrol/AuNP composites deposited by different electrochemical methods: sensing properties towards catechol. Beilstein J Nanotechnol 6:2052–2061
30. Ghadimi H, Mahmoudian MR, Basirun WJ (2015) A sensitive dopamine biosensor based on ultra-thin polypyrrole nanosheets decorated with Pt nanoparticles. RSC Adv 5:39366–39374
31. Turco A, Mazzotta E, Di Franco C, Santacroce M, Scamarcio G, Monteduro A, Primiceri E, Malitesta C (2016) Templateless synthesis of polypyrrole nanowires by non-static solution-surface electropolymerization. J Solid State Electrochem 20(8):2143–2151
32. Tang Y, Cheng W (2012) Metallic nanoparticles as advanced electrocatalysts. Sci Adv Mater 4:784–797
33. Niu L, Li Q, Wei F, Wu S, Liu PCX (2005) Electrocatalytic behavior of Pt-modified polyaniline electrode for methanol oxidation: effect of Pt deposition modes. J Electroanal Chem 578:331–337
34. Stoychev D, Papoutsis A, Kelaidopoulou A, Kokkinidis GMA (2001) Electrodeposition of platinum on metallic and nonmetallic substrates—selection of experimental conditions. Mater Chem Phys 72:360–365
35. Malitesta C, Losito I, Sabbatini L, Zambonin PG (1995) New findings on polypyrrole chemical structure by XPS coupled to chemical derivatization labelling. J Electron Spectros Relat Phenomena 76: 629–634
36. Buitrago-Sierra R, García-Fernández MJ, Pastor-Blas MM, Sepúlveda-Escribano A (2013) Environmentally friendly reduction of a platinum catalyst precursor supported on polypyrrole. Green Chem 15:1981
37. Vercelli B, Zotti G, Berlin A (2009) Mono- and multilayers of platinum nanoparticles and poly(3,4- ethylenedioxythiophene) as nanostructures for methanol electroxidation. J Phys Chem C 113: 3525–3529
38. Ribeiro JA, Fernandes PMV, Pereira CM, Silva F (2016) Electrochemical sensors and biosensors for determination of catecholamine neurotransmitters: a review. Talanta 160:653–679
39. Bishop E, Hussein W (1984) Anodic voltammetry of dopamine, noradrenaline and related compounds at rotating disc electrodes of platinum and gold. Analyst 109:627–632
40. Austin DS, Polta JA, Polta TZ, Tang APC, Cabelka TD, Johnson DC (1984) Electrocatalysis at platinum electrodes for anodic electoanalysis. J Electroanal Chem Interfacial Electrochem 168: 227–248
41. Bose CSC, Rajeshwar K (1992) Efficient electrocatalyst assemblies for proton and oxygen reduction: the electrosynthesis and characterization of polypyrrole films containing nanodispersed platinum particles. J Electroanal Chem 333:235–256
42. Gholamian M, Contractor AQ (1990) Oxidation of formic acid at platinum microparticles dispersed in a polyaniline matrix. Influence of long-range order and metal-polymer interaction J Electroanal Chem 289:69–83
43. Ghanbari K, Hajheidari N (2015) Simultaneous electrochemical determination of dopamine, uric acid and ascorbic acid using silver nanoparticles deposited on polypyrrole nanofibers. J Polym Res 22: 152
44. Lin M (2015) A dopamine electrochemical sensor based on gold nanoparticles/over-oxidized polypyrrole nanotube composite arrays. RSC Adv 5:9848–9851
45. Ding J, Zhang K, Wei G, Su Z (2015) Fabrication of polypyrrole nanoplates decorated with silver and gold nanoparticles for sensor applications. RSC Adv 5:69745–69752
46. Karazehir T, Gokce ZG, Ates M, Sarac AS (2017) Gold nanoparticle/nickel oxide/poly(pyrrole-N-propionic acid) hybrid multilayer film: electrochemical study and its application in biosensing. Express Polym Lett 11:449–466
47. Zhang H, Zhang F, Li S, Li H (2017) A multilayer gold nanoparticle-polydopamine hybrid membrane-modified indium tin oxide electrode for selective sensing of dopamine in the present of ascorbic acid. Ionics (Kiel)
48. Choudhary M, Brink R, Nandi D, Siwal SMK (2017) Gold nanoparticle within the polymer chain, a multi-functional composite material, for the electrochemical detection of dopamine and the hydrogen atom-mediated reduction of Rhodamine-B, a mechanistic approach. J Mater Sci 52:770–781

49. Chen T, Tang L, Yang F, Zhao Q, Jin X, Ning YZG (2016) Electrochemical determination of dopamine by a reduced graphene oxide–gold nanoparticle-modified glassy carbon electrode. Anal Lett 49:2223–2233
50. Li D, Ao K, Wang Q et al (2016) Preparation of Pd/bacterial cellulose hybrid nanofibers for dopamine detection. Molecules 21:1–11
51. Sun L, Li H, Li M, Li P, Li CYB (2016) Simultaneous determination of small biomolecules and nitrite using an Au/TiO 2 /carbon nanotube composite-modified electrode. J Electrochem Soc 163: B567–B572
52. Palanisamy S, Thirumalraj B, Chen S, Ali MA-HF (2015) Palladium nanoparticles decorated on activated fullerene modified screen printed carbon electrode for enhanced electrochemical sensing of dopamine. J Colloid Interface Sci 448:251–256
53. Nayak P, Santhosh PN, Ramaprabhu S (2015) Cerium oxide nanoparticles decorated graphene nanosheets for selective detection of dopamine. J Nanosci Nanotechnol 15:4855–4862
54. Ardakani MM, Talebi A, Naeimi H, Barzoky MN, Taghavinia N (2009) Fabrication of modified TiO2 nanoparticle carbon paste electrode for simultaneous determination of dopamine, uric acid, and l-cysteine. J Solid State Electrochem 13:1433–1440